University of Chicago

PHYSICS 575

A MULTI TeV $e^+ e^-$ LINEAR COLLIDER BASED ON CLIC TWO BEAM ACCELERATION TECHNOLOGY*

Wei Gai

Advanced Accelerator R&D
High Energy Physics Group
Argonne National Laboratory

March 7, 2002

***This lecture is prepared based on the published reports and materials from CLIC study team. In this lecture, we introduce the basic concepts of achieving multi TeV collider using Compact LInear Collider (CLIC) scheme. The core materials are covered in section 2, 3.1, 3.5, 3.6. This lecture has no homework assignment.**

1. Introduction

As at other accelerator laboratories, the top priorities at CERN in the 21st century will be experiments probing beyond the Standard Model [1.1]. Indeed, this is surely the only responsible motivation for major new accelerators [1.2].

A high-energy (0.5–5 TeV centre-of-mass), high-luminosity (10^{34}–10^{35} cm^{-2} s^{-1}) e+ e^{-} Compact Linear Collider (CLIC) is being studied at CERN [1.3], [1.4] as a possible new high-energy physics facility for the post-LHC era [1.5]. The maximum energy of 5 TeV is well above those presently being proposed by other linear collider studies. The physics experiments require a luminosity of at least 10^{34} cm^{-2} s^{-1} at 1 TeV c.m. and this luminosity should increase at higher energies [1.4]. Although the design study has been optimized for 3 TeV centre of mass, the collider could start operation at a lower energy and then be upgraded in stages. The design is such that these upgrades can be made without major modifications. CLIC is based on the Two-Beam Acceleration (TBA) method in which the RF power for sections of the main linac is extracted from a secondary, low-energy, high-intensity electron beam running parallel to the main linac. The power is extracted from the beam by special Power Extraction and Transfer Structures (PETS). For a 3 TeV collider, there are 22 such drive-beams, each of which provides enough power to accelerate the main beam by ~70 GeV. All the drive-beams are generated in a centrally located facility. The only difference between the drive-beam generation schemes for high and low colliding beam energies is the length of the modulator pulse (the installed hardware is exactly the same). This means that the entire drive-beam generation system has to be installed in the first stage. The overall layout of CLIC is sketched in Fig. 1.1. Two interaction points (IPs) are foreseen, one for e + –e – and one for γ–γ. For a c.m. energy of 3 TeV and an accelerating gradient of 150 MV/m, and allowing ~10 km for the Beam Delivery (BD) area, CLIC would cover a total length of approximately 38 km. In this note, we only concentrate on the acceleration of the main beams (see the upper half of Fig. 1.1). The main part of this lecture is to study the

drive-beam complex, and the production of 30 GHz RF power (see the lower half of Fig. 1.1) is presented in Section 3.

Overall layout of the CLIC scheme is shown in Figure 1 and basic parameters are shown in Table 1.

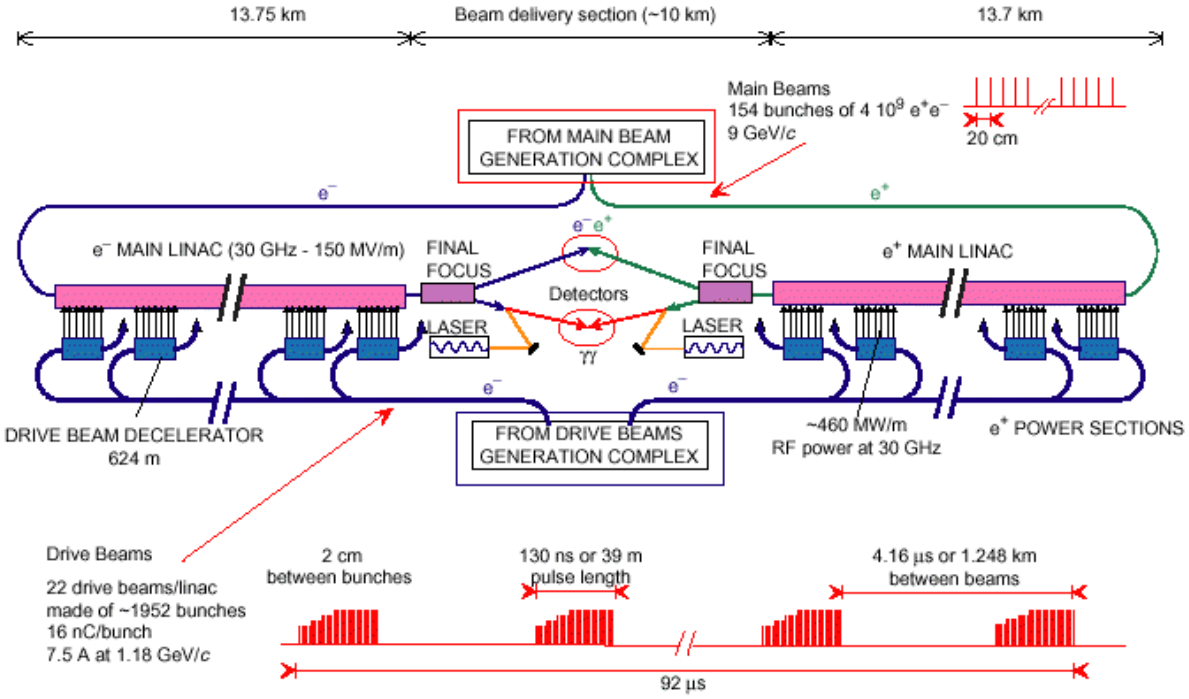

Figure 1.1 Overall layout of the CLIC scheme

Among the different technological ways of building a linear collider, the CLIC study explores the technical feasibility of two-beam acceleration using high-frequency, room-temperature, and travelling-wave structures. A high RF frequency has been chosen in order to be able to operate at a high accelerating gradient which reduces the length, and in consequence, the cost of the linacs. The choice of 30 GHz is considered to be close to the limit beyond which standard technology for the fabrication of accelerating structures can no longer be used. The main drawback of operating at a high RF frequency is that the accelerator iris aperture is very small (~4 mm), leading to the generation of strong wakefields and the related dilution of the transverse emittance. The effects of these strong wakefields can be minimized by a judicious choice of beam and linac parameters. These parameters have been optimized using general scaling laws derived from linear collider

studies covering more than a factor 10 in frequency. The resulting main-beam and linac parameters corresponding to CLIC at 3 TeV c.m. are listed in Table 1

Main-beam parameters at IP		
Luminosity (with pinch)	L	10.0×10^{34} cm^{-2} s^{-1}
Luminosity (in 1% of energy)	$L_{1\%}$	3.0×10^{34} cm^{-2} s^{-1}
Beamstrahlung mom. spread	δ_B	31%
Beamstrahlung parameter	Y	8.1
Number of photons/electron	N_γ	2.3
Number of particles/bunch	N_b	$4.0 \times 10^9 e^{\pm}$
Number of bunches/pulse	k_b	154
Bunch spacing	Δ_b	20 cm
	Δt_b	0.666 ns
Transverse emittances	$\gamma\varepsilon_{x/y}$	680/20 nm·rad
Beta functions	$\beta_{x/y}$	8/0.15 mm
r.m.s. beam size (no pinch)	$\sigma_{x/y}$	43/1 nm
Bunch length	σ_z	30 μm
Enhancement factor	H_D	2.24
Beam power per beam	P_b	14.8 MW
Main-linac parameters		
Centre-of-mass energy	E_{CM}	3 TeV
Linac repetition rate	f_{rep}	100 Hz
RF frequency of linac	$\omega/2\pi$	30 GHz
Acceleration field (loaded)	G_a	150 MV/m
Energy overhead		8%
Active length per linac	L_A	10.74 km
Total two-linac length	L_{tot}	27.5 km
RF power at structure input	P_{st}	229 MW
RF pulse duration	Δt_p	102 ns
Number of drive-beams/linac	N_D	22
Number of structures per linac		21 470
AC-to-RF efficiency	η_{RF}^{AC}	40.3%
RF-to-beam efficiency	η_b^{RF}	24.4%
AC-to-beam efficiency	η_b^{AC}	9.8%
AC power for RF production	P_{AC}	300 MW

Reference:

[1.1] J. Ellis, Physics goals of the next century at CERN, CERN-TH-2000–050 (2000).
[1.2] The Physics Study Group for CLIC, http://clicphysics.web.cern.ch/CLICphysics/
[1.3] J.-P. Delahaye et al., The CLIC study of a multi-TeV e + e – linear collider, Proc. Part. Accel. Conf. (PAC99), New York, 1999, Eds. A. Luccio and W. MacKay (IEEE Computer Soc. Press, Piscataway, N. J., 1999).
[1.4] International Linear Collider Technical Review Committee Report, Ed. G. Loew, SLAC-R-95–471 (1995). http://www.slac.stanford.edu/pubs/slacreports/slac-r-471.html
[1.5] J. Ellis, E. Keil and G. Rolandi, Options for future colliders at CERN, CERN-EP/98–03, CERN-SL 98–004 (AP) and CERN-TH/98–33 (1998). http://preprints.cern.ch/cgi-bin/setlink?base=preprint&categ=cern&id=SL-98-004

2. Main Linac

The CLIC main linac accelerating structure, the Tapered Damped Structure (TDS), has 150 cells, is 500 mm long, and operates in the $2\pi/3$ travelling-wave mode. The design of the structure is driven by extreme performance requirements: accelerating gradients well in excess of 150 MV/m, power flows in excess of 200 MW, a 10 μm structure straightness and alignment tolerance (to preserve single-bunch emittance), long-range transverse wakefield suppression of over two orders of magnitude (to preserve train emittance) and ultimately a low mass-production cost.

The issues of gradient, power and tolerances are each in part addressed by ultrahigh precision diamond turning of the copper disks that make up the sections. This technique gives a 1–2 μm dimensional tolerance and an optical-quality surface finish. The 10 μm tolerance of assembled sections is guaranteed by a specially developed hybrid brazing/diffusion bonding technique. Measured *Q* factors correspond to 98% of the theoretical value in (undamped) constant impedance structures. Constant impedance structures were tested in CTF1 to 125 MV/m (albeit with pulses that reached these peak levels for only a few nanoseconds). [2.1]

Unlike SLAC's RDDS structures, the long-range transverse wakefields are suppressed through a combination of strong damping and detuning. The damping is accomplished by coupling to each cell of the structure four individually terminated waveguides. The damping waveguides have a rectangular cross-section of 4.5 mm by 1.9 mm, hence a cutoff frequency of 33.3 GHz, which is above the fundamental but below all higher-order modes. In this way higher-order mode energy propagates out of the cells via the damping waveguides but the fundamental mode energy does not. This results in a *Q* of approximately 16 for the lowest, and most dangerous, dipole passband. A taper in the iris diameter from 4.5 mm at the head of the structure to 3.5 mm at the tail provides a detuning frequency spread of 2 GHz (5.4%).

The layout of the cell structure can be seen in Figs. 2.1 and 2.2.

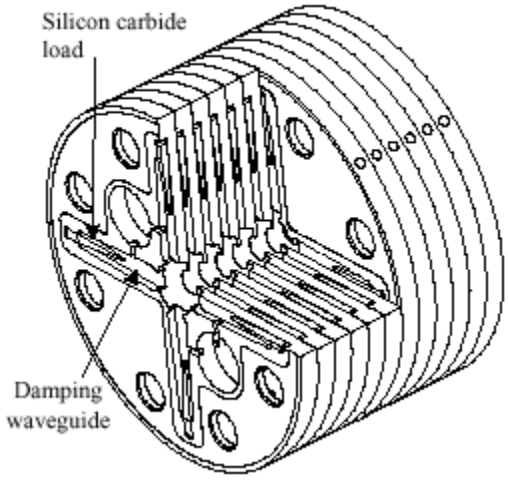

Fig. 2.1: *Cross-sectional view of the TDS geometry.*

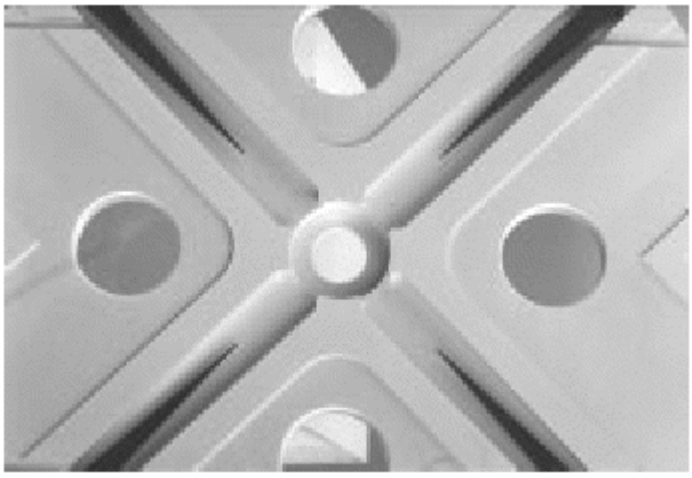

Fig. 2.2: *Photograph of a TDS cell with damping waveguides and SiC loads.*

The acceleration scheme using a drive beam traveling in parallel with the main accelerator is shown in Figure 2.3. Detailed descriptions of the drive beam decelerator are discussed in the next section, which is main part of this lecture.

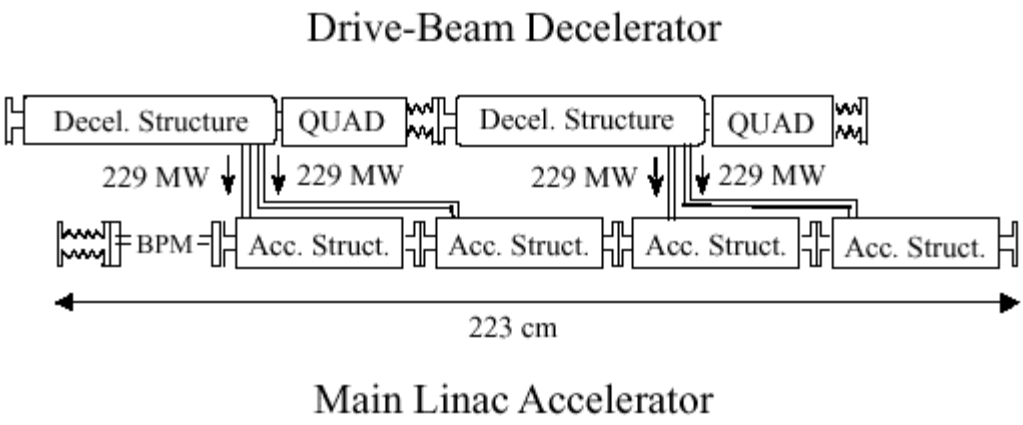

Figure 2.3 A main linac accelerator module.

Reference:

[2.1] M. Dehler, I. Wilson and W. Wuensch, A tapered damped accelerating structure for CLIC, Proc. 19th Int. Lin. Accel. Conf. (LINAC'98), Chicago, 1998, URL:http://www.aps.anl.gov/conferences/LINAC98/papers/TH4083.pdf

3 Drive Beam and RF Power Source

3.1 Introduction

The CLIC study focuses on high-gradient, high-frequency (30 GHz) acceleration for multi-TeV linear colliders. Short RF pulses of high peak power are typically required in high-frequency linear colliders. In the case of CLIC, 130 ns long pulses at about 230 MW per accelerating structure are needed, but no conventional RF source at 30 GHz can provide such pulses. This leads naturally to the exploration of the two-beam acceleration technique as initially proposed by Sessler[3.1], in which an electron beam (the drive beam) is accelerated using standard, low-frequency RF sources and then used to produce RF power at high frequency.

In linear collider projects based on conventional RF sources (klystrons), pulse compression or delayed distribution techniques are used in order to obtain the needed high peak power and short pulse length. Similar techniques can be used in two-beam accelerators. In the CLIC case, however, the compression and distribution are done with electron beams [3.2]. The main advantage of electron beam manipulation, with respect to manipulation of RF pulses, consists in the very low losses that can be obtained while transporting the beam pulses over long distances and compressing them to very high ratios. A further advantage is the possibility of frequency multiplication, achieved by interleaving bunched beams by means of transverse RF deflectors [3.3]. In the following we will describe the CLIC RF power source complex used to generate all the RF power needed for one of the two main linacs (electron or positron). Possibilities to combine some elements of both the e + and e – complexes are under study. A schematic layout of one complex is shown in Fig. 3.1.

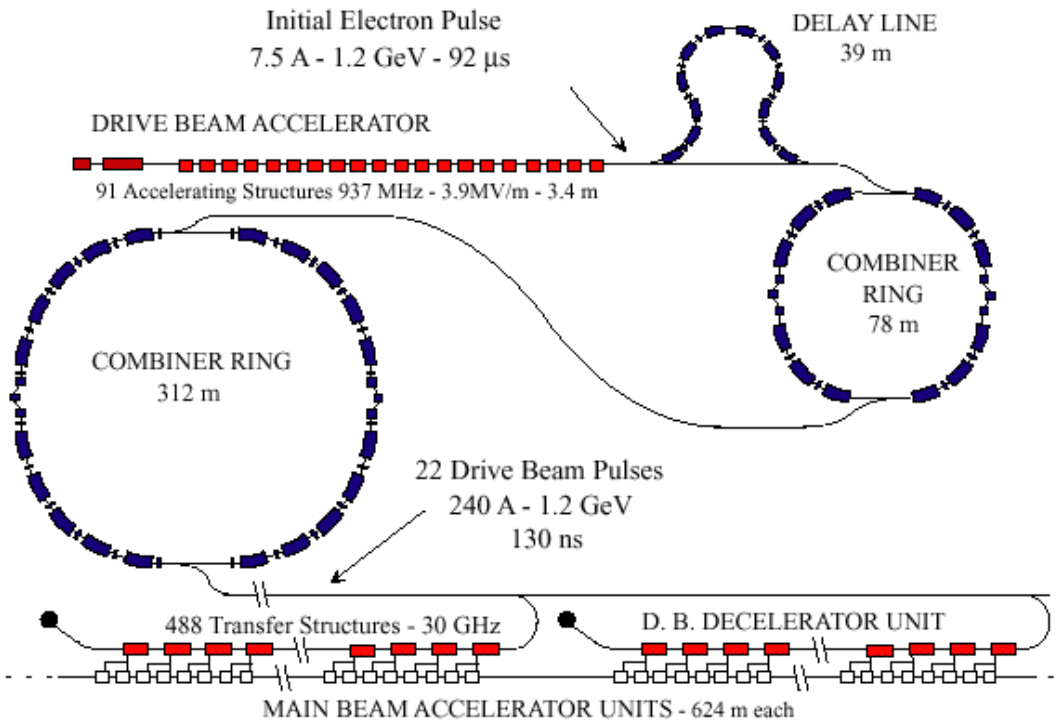

Fig. 3.1: *Schematic layout of the CLIC RF power source. Two such complexes (one for each of the main linacs) will be needed to provide the power for 3 TeV c.m. CLIC operation. Only two of the 22 decelerator/accelerator units composing a linac are shown.*

The CLIC RF power source can be thought of as a 'black box' that combines and transforms several long, low-frequency RF pulses into many short, high-power pulses at high frequency. During the process, the energy is stored in a relativistic electron beam, which is manipulated in order to obtain the desired time structure and then transported to the place where the energy is needed. The energy is finally extracted from the electron beam in resonant decelerating structures, which run parallel to the main accelerator and are called Power Extraction and Transfer Structures (PETS).

The key points of the system are an efficient acceleration of the drive beam in conventional structures, the introduction of transverse RF deflectors to manipulate the drive beam, and the use of several drive-beam pulses in a counter-flow distribution system, each one powering a different section of the main linac.

The primary characteristic of this scheme consists of using the energy stored in different time bins of a long electron-beam pulse to create the RF necessary for different sections of a long linac. Thus, the same accelerator and beam manipulation system is used to create all the beam pulses needed for powering one of the two main linacs. The method discussed here seems relatively inexpensive, very flexible and can be applied to the beam-acceleration in various linear colliders over the entire frequency and energy range applicable.

The drive-beam generation complex is located at the centre of the linear collider complex, near the final-focus system. The energy for the RF production is initially stored in a 92 μs long electron beam pulse (corresponding to twice the length of the high-gradient, main linac) which is accelerated to about 1.2 GeV by a normal-conducting, low-frequency (937 MHz) travelling wave linac. The linac is powered by conventional long-pulse klystrons. A high-energy transfer efficiency is paramount in this stage. The drive beam is accelerated in relatively short structures (3.4 m long), such that the RF losses in the copper are minimized. Furthermore, the structures are fully beam-loaded, i.e., the accelerating gradient is zero at the downstream end of each structure and no RF power flows out to a load. In this way, about 98% of the RF energy can be transferred to the beam. The beam pulse is composed of 32×22 subpulses, each one 130 ns long. In each subpulse the electron bunches occupy alternately even and odd buckets of the drive-beam accelerator fundamental frequency (937 MHz). Such a time structure is produced after the thermionic gun in a subharmonic buncher, whose phase is rapidly switched by 180° every 130 ns. This type of pulse train can also be produced using a RF photocathode. This provides us with a means to separate the subpulses after acceleration, while keeping a constant current in the accelerator and avoiding transient beam-loading. With nominal phase-switching times, the resulting pulse of the acceleration voltage is rectangular. By delaying the phase-switching time, it is also possible to obtain subpulses of different lengths. When the different subpulses are superimposed at the end of the combination process, one can thus obtain a current ramp of about 22 ns at the leading edge of the pulse. This in turn produces a ramp in the PETS power output, which is used for beam-loading compensation in the main linac. An illustration of this technique is given in Fig. 3.2 under the assumption that only one combiner ring is used, folding the beam by a

factor two only. If the phase-switching is delayed after the first two trains, the shape of the voltage pulse is not flat anymore. The trailing bunches which are located after the nominal switching time add to the train considered and consequently append to the tail of the final pulse. In the train which follows the delayed switching, the first few bunches are missing and this generates gaps at the head of the final pulse. This results in a variation of the density of bunches and therefore in a ramp of the current. The unwanted tail is of no concern since it goes through the drive-beam decelerator after the passage of the main beam.

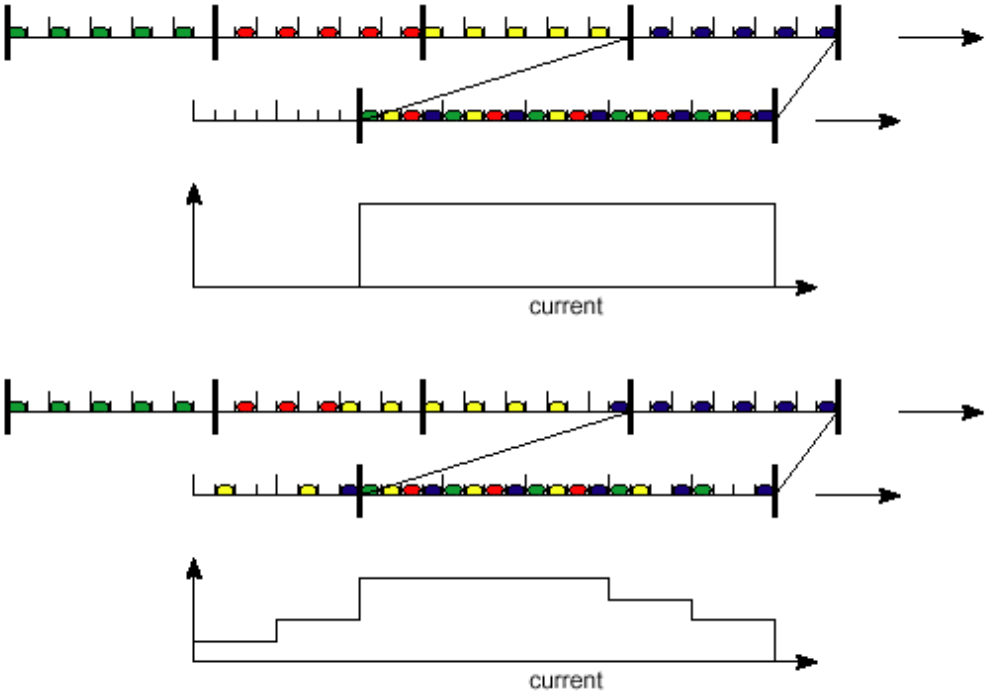

Fig. 3.2: *Illustration of the delayed switching scheme. In the upper case, the phase is switched at nominal times, creating a rectangular pulse. In the lower case, the phase shift is delayed in order to create a ramp of beam current.*

As the long pulse leaves the drive-beam accelerator, it passes through a delay-line combiner [3.2] where ‘odd’ and ‘even’ subpulses are separated by a transverse RF deflector at the frequency of 468.5 MHz. Each ‘even’ bunch train is delayed with respect to the following ‘odd’ one by 130 ns. The subpulses are recombined two-by-two by interleaving the electron bunches in a second RF deflector at the same frequency. The net effect is to convert the long pulse to a periodic sequence of drive-beam pulses with gaps in between. After recombination, the pulse is composed of 16×22 subpulses (or trains)

whose spacing is equal to the train length. The peak power and the bunch frequency are doubled.

The same principle of electron-bunch pulse combination is then used to combine the trains four-by-four in a first combiner ring, 78 m long. Two 937 MHz RF deflectors create a time-dependent local deformation of the equilibrium orbit in the ring. This bump is used for injection of a first train in the ring (all its bunches being deflected by the second RF deflector onto the equilibrium orbit). The ring length is equal to the spacing between trains plus l/4, where λ is the spacing between bunches, equal to the wavelength of the RF deflectors. Thus, for each revolution period, the RF phase seen by the bunches circulating in the ring increases by 90°, and when the second train is injected, the first one does not see any deflection and its bunches are interleaved with the ones which are injected (at a l/4 distance). This is repeated twice, then the four interleaved trains are extracted from the ring by an ejection kicker half a turn later, and the same cycle starts again. After the first combiner ring the whole pulse is composed of 4×22 trains.

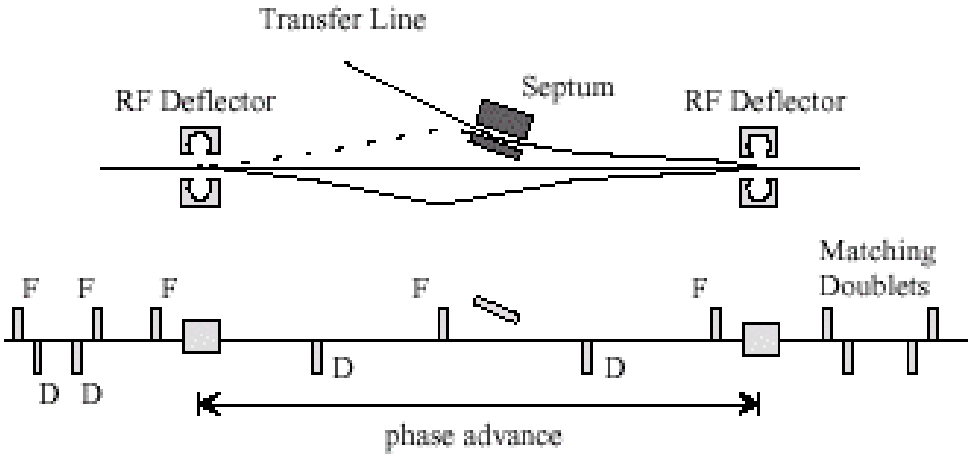

Figure 3.3 *Rf deflectors and transfer line. It shows how beams can be combined.*

The trains are combined again, using the same mechanism, in a second combiner ring, 312 m long, yielding another factor four in frequency multiplication, and obtaining

the final 22 trains required for the main linac. At this point, each final train is 39 m long and consists of 1952 bunches with a charge of 16 nC/bunch and an energy of 1.18 GeV.

Such drive-beam pulses are distributed down the main linac via a common transport line, in a direction opposite to the direction of the main beam. The distance between trains is now 1248 m, corresponding to twice the length of the linac section which they will power, so that they will arrive at the appropriate time to accelerate a high-energy beam travelling in the opposite direction.

Pulsed magnets deflect each beam at the appropriate time into a turn-around. After the turn-around each pulse is decelerated in a 624 m long sequence of low-impedance Power Extraction and Transfer Structures (PETS) down to a minimum energy close to 0.12 GeV (Fig. 3.22), and the resulting output power is transferred to accelerate the high-energy beam in the main linac. As the main beam travels along, a new drive-beam train periodically joins it and runs in parallel but ahead of it to produce the necessary power for a 624 m long linac unit. At the end of a unit the remaining energy in the drive beam is dumped while a new one takes over the job of accelerating the main beam. The main characteristics of one drive-beam unit are given in Table 3.1.

Table 3.1: Main parameters of a drive-beam unit

Parameter	Symbol	Value
Drive-beam pulse		
Energy (initial)	$E_{\mathrm{in,dec}}$	1.18 GeV
Energy (final, minimum)	$E_{\mathrm{fin,dec}}$	118 MeV
Current	I_{dec}	240 A
Pulse duration (FWHH)	τ_{train}	130 ns
Charge/train	Q_{train}	31.25 μC
Total energy/train	W_{train}	36.9 kJ
Number bunches/train	$N_{\mathrm{b,dec}}$	1952
Bunch charge	$Q_{\mathrm{b,dec}}$	16 nC
Bunch separation	$\Delta_{\mathrm{b,dec}}$	0.067 ns
Bunch length, r.m.s.	$\sigma_{\mathrm{z,dec}}$	0.4 mm
Normalized emittance, r.m.s. (injection)	$\varepsilon_{\mathrm{n,dec}}$	150 μm·rad
Decelerator unit		
Repetition rate	f_{rep}	100 Hz
Unit length (total)	$L_{\mathrm{unit,tot}}$	624 m
Unit length (active)	$L_{\mathrm{unit,act}}$	390 m
Number of PETS/unit	$N_{\mathrm{PETS,unit}}$	488
Number of quadrupoles/unit	$N_{\mathrm{quad,unit}}$	488
Decelerating gradient	G_{dec}	2.8 MV/m
Power extracted/metre	P_{out}	458 MW
Main beam energy gain/unit	ΔE_{main}	68 GeV

3.

3.2 Drive-beam Generation

The basic scheme for the drive-beam injector has been further developed and adapted to the new parameter set. The total pulse, at the injector exit, is 92 μs (Fig. 3.4) and is composed of 32×22 subpulses as mentioned in Section 3.1. The time structure of this pulse is produced after the thermionic gun in a subharmonic buncher, in such a way that the electron bunches of each subpulse occupy alternately even and odd buckets (Fig. 3.4). This is indeed the requisite for subsequent separation of the subpulses, and their recombination in the combiner rings.

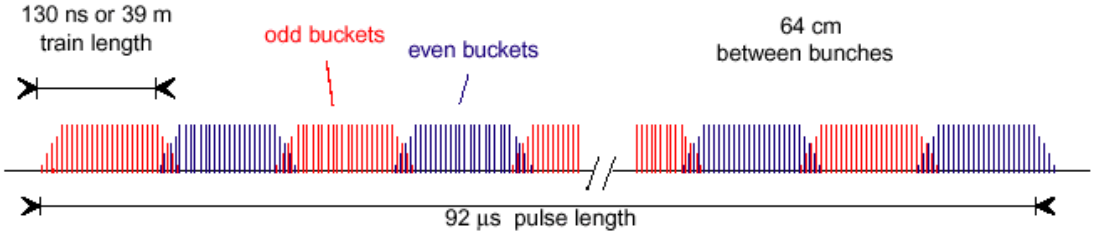

I

Fig. 3.4 : *Combined pulses at the injector exit or linac entrance.*

3.2.1. Thermionic gun

There is a design for thermoionic based injector design study. We skip it here due to space and time limitation. Interested student should read the CLIC report for details.

3.2.2 RF photocathode based system

The possibility to use a RF photo-injector as the drive-beam source is under investigation. Figure 3.5 gives a sketch of a possible layout. A CW laser working at 468.5 MHz provides a continuous train. During 92 μs the necessary power at 262 nm is generated in order to create the charge of 750 μC by the photocathode. The 'even' and 'odd' photon pulses are directly produced by electro-optics components. The resulting laser beam illuminates the photocathode of an RF gun powered by a klystron at 937 MHz. It generates an electron beam with a momentum of several MeV at the exit of the photo-injector and with the required sequence of bunches which can then be directly injected into the drive-beam accelerating linac. Such an option would represent several advantages: it would replace the thermionic gun and the bunching system by a single RF

gun; the pulse shaping would be much easier and could be adjusted in order to optimize the RF power generation; small emittances would be achievable. However, several issues remain to be addressed: the UV power and stability for the laser and the necessary charge for the photocathodes. An R&D program has been set up to try to overcome these problems. Currently, the Argonne Wakefield accelerator group is also studying RF photocathode option.

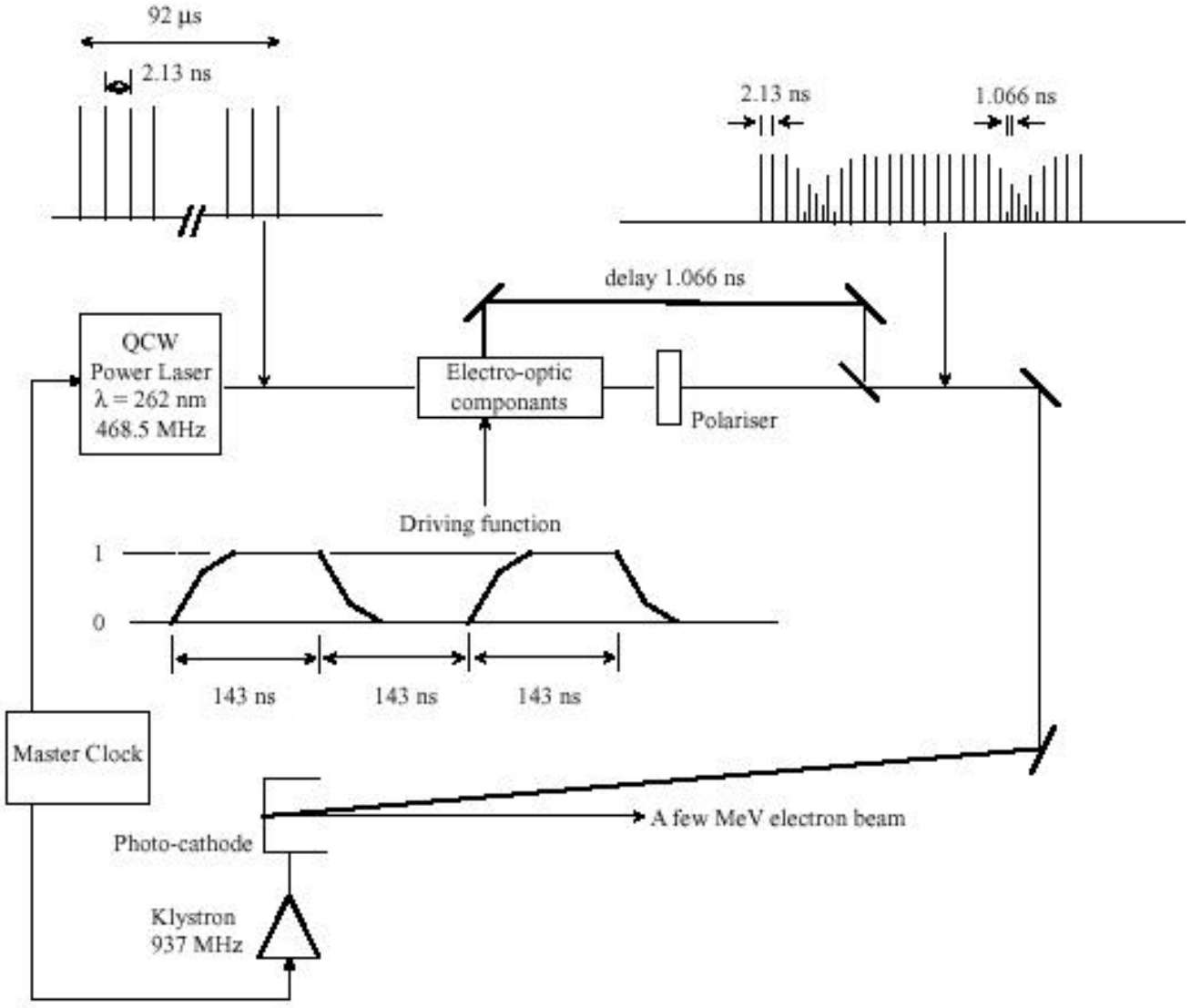

Fig. 3.5 : Possible layout for a photo-injector option.

3.3 Drive-beam accelerating linac

3.3.1 The accelerator beam dynamics

The drive-beam accelerator is accelerated from 50 MeV to about 1.2 GeV. Every second bucket of the beam is filled with a charge of about 16 nC, switching from odd to even buckets or vice versa every 60 bunches. For the simulation the single-bunch wakefields were derived from the ones calculated for SBLC [3.6] by scaling with the frequency and iris radius. The longitudinal multibunch wakefields were ignored, their effect should be small due to the beam loading compensation scheme. The transverse wakefields were calculated for a constant impedance structure for four different iris radii [3.7]. For each cell the loss factor and the frequency of the two most important dipole modes were derived by interpolation. An analysis that includes the coupling between cells and the damping remains to be done. Conservatively, a damping with $Q = 100$ was assumed for the first dipole mode and with $Q = 400$ for the second.

The initial bunch length in the accelerator is $\sigma_z = 4$ mm while in the decelerator it should be smaller than 0.4 mm. Therefore, bunch compression is needed. On the other hand, the bunch length has to be larger than 2 mm in the combiner rings and the following bends in order to suppress coherent synchrotron radiation. Thus a final compression is needed at the point where the beam is bent into the decelerator. To evaluate the final bunch length a simple calculation was performed [3.8]. The compression stages are assumed to be linear. Two different strategies of compression exist. One can compress the beam to $\sigma_z = 2$ mm at about $E = 100$ MeV and then just accelerate it. The final compression after the final bends then yields a bunch length of $\sigma z = 290$ μm. It is also possible to compress the beam as much as possible at three stages in the linac. Before the rings the beam is uncompressed to $\sigma z = 2$ mm. After the final bend it is compressed as much as possible yielding $\sigma z = 170$ μm.

3.3.2 Description of the accelerator cavities

3.3.2.1 Structure description and scaling

The group velocities and the *R'/Q* values must be such as to enable the beam to use up properly the electromagnetic energy before it reaches the structure end. Two

possible designs of the accelerator cavities are being investigated. A new concept based on a slotted iris and constant aperture is proposed (E. Jensen et al., LINAC 2000). The model based on a classical geometry in order to avoid excessive surface gradients is described below.

First beam transport simulations with 937 MHz structures of 29 cells having an average iris radius a equal to 48.5 mm, an average outer radius b = 144 mm and a disc thickness d = 19 mm demonstrated that both detuning and damping were necessary to preserve a sufficiently low transverse beam emittance. The design is based on the same principles proposed for the CLIC main accelerating structures [2.1]. Good beam transmission was obtained with a dipole frequency spread of about 10% and a Q-value of 100 for the first mode and 400 for the second one (see Section 3.3.1 on beam dynamics). Since some scaled model work was planned at 3 GHz, the investigations with the code ABCI were all done for structures with this fundamental frequency (the average iris radius a scales to 15 mm at 3 GHz). A 29-cell structure having for the first cell a = 17 mm and for the last one a = 13.3 mm was used.

Table 3.1 lists the relevant parameters of the two extreme cells for zero bunch length and the 937 MHz operating frequency of the CLIC drive beam.

Table 3.4: Parameters of the first and last cell of the 937 MHz structure

Quantity	First cell	Last cell	Units
Iris radius a	54.4	42.6	mm
Relative group velocity v_g	0.053	0.025	–
Outer radius b	147.2	140	mm
R/Q for fundamental mode	1088	1340	Ω/m (linac)
Frequency of first transverse mode	1.22	1.34	GHz
Transverse loss factor k of first mode	32.34	63.5	V/pC/m^2
Frequency of second transverse mode	2.14	2.18	GHz
Transverse loss factor k of second mode	3.1	13.7	V/pC/m^2

A 32-cell damped, detuned scale-model has been realized for 3 GHz (Fig. 3.6). Damping was confirmed by computations on a single cell using the HFSS code yielding Q-values of 11 and 100 for the first and second transverse modes, respectively. The

model work and the HFSS calculations have demonstrated that sufficient damping for beam survival is obtainable.

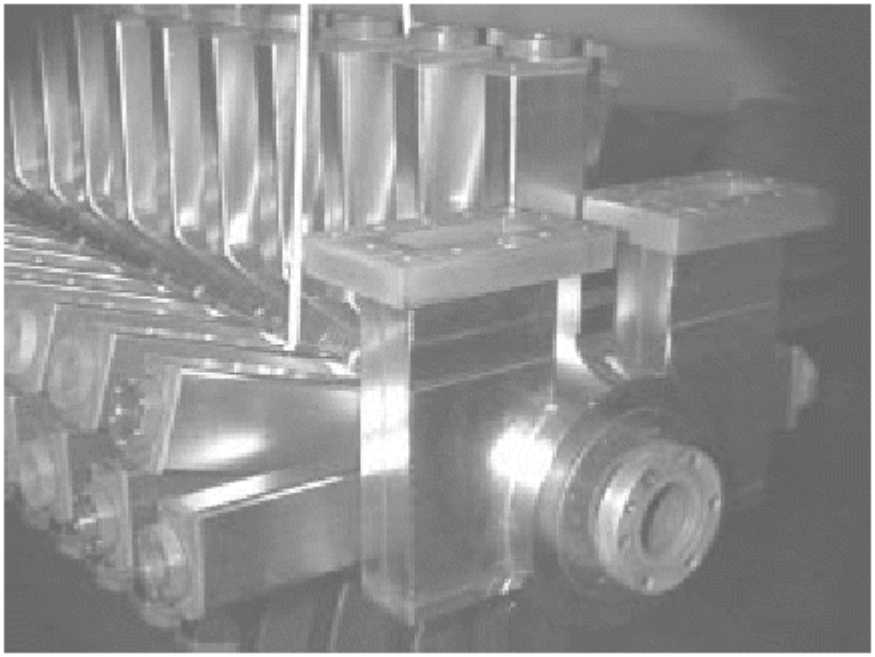

Fig. 3.6: *Front end of a 3 GHz scaled CLIC drive-beam acceleration structure with transverse damping waveguides against bipolar and quadrupolar high-order modes. Each such waveguide contains a SiC absorber.*

3.3.3 Drive-beam power systems

3.3.3.1 Klystrons

The CLIC drive-beam RF power system provides 100 MW, 100 μs long pulses for each single accelerating structure of the 1.2 GeV, fully loaded and conventional 937 MHz, L-band linac [3.2]. A modular drive power system approach has been chosen, where the RF outputs from two 50 MW klystrons are connected to this single 3.4 m long, traveling wave structure, via 3 dB power combiners.

3.4 Frequency multiplication and pulse compression

3.4.1 Design of the delay line and combiner rings

The main issue in the compression system (delay line plus combiner rings) is the preservation of the bunch quality during the combination process. In particular, the bunch length and longitudinal phase-space distribution must be preserved and the fluctuations in phase and transverse position between trains and between bunches minimized.

The rings, the delay line and the transfer lines must therefore be isochronous. The final bunch length must be short in order to maximize the 30 GHz RF power production efficiency in the drive-beam decelerator. The aim is an r.m.s. bunch length of $\sigma z = 0.4$ mm, for a 16 nC bunch-charge. High-charge, short bunches can radiate a considerable amount of Coherent Synchrotron Radiation (CSR), leading to both a significant average energy-loss and energy-spread within the bunch [3.15]. The emission is concentrated at low frequencies [$\nu \leq 1/(2\ s)$], and can be partly suppressed if at least a fraction of the emitted spectrum is below the cut-off of the beam pipe (shielding effect), though a lower limit in the beam pipe dimensions is imposed by the necessary beam clearance. Both the energy loss and spread must be kept small, in particular because the bunches belonging to different trains make a different number of turns in the rings (from 1/2 to 7/2) and will develop different energy distributions. This will cause relative phase errors between bunches and some bunch lengthening. These intense and short bunches will also interact with any small discontinuity of the beam chamber (e.g., bellows and septa), possibly being subject to longitudinal and transverse wakefields. It is therefore highly desirable to have relatively long bunches to manipulate in the compression system, and to compress them just before the injection into the drive-beam decelerator sections. An upper limit to the bunch length is given by the non-uniform kick experienced by the bunches at injection in the RF deflectors, due to their phase extension, causing growth of the single-bunch emittance. The bunch length has been fixed at the exit of the accelerator to be 2 mm r.m.s. approximately. The emittance growth in this case is approximately 2% (for an initial r.m.s. normalized emittance of 200 mμ×rad), arising mainly in the deflectors (3.75 GHz) of the second combiner ring, where their effect is large. A correlated energy spread (~1% r.m.s.), suitable for the final bunch compression, is obtained in the accelerator by the combined effect of the RF curvature and longitudinal wakefields. The need to preserve the correlation all along the compression system means that all the distortions of the longitudinal phase space must be kept small. In particular, attention must be given to the higher orders of the momentum compaction. A numerical analysis has shown that second-order effects would be unacceptable and must be corrected by using sextupoles [3.2].

3.5 Drive-beam decelerator

3.5.1 The Power Extraction and Transfer Structure

3.5.2.1 Definition and function of the PETS

The Power Extraction and Transfer Structure (PETS) [3.26] is a passive microwave device in which the bunches of the drive beam interact with the impedance of periodically loaded waveguides and excite preferentially the synchronous hybrid TM mode at 30 GHz. In the process, the beam kinetic energy is converted into electromagnetic energy at the mode frequency, which travels along the structure with the mode group velocity. The microwave power produced is collected at the downstream end of the structure by means of couplers and conveyed to the main linac accelerating structures by means of rectangular waveguides [3.27]. In its classic configuration, the PETS consists of a cylindrical beam chamber, which is coupled by longitudinal slits to four teeth-loaded waveguides as visible in Fig. 3.7, which shows the PETS model with beam chamber diameter 26 mm.

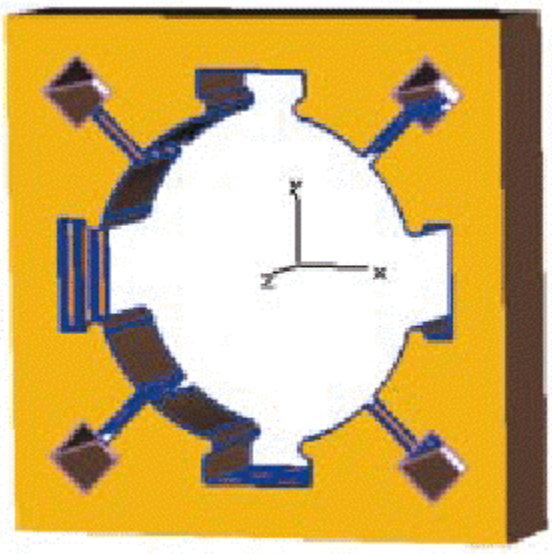

Fig. 3.7: *Four-waveguide PETS.*

3.5.2.2 Principle of operation

When a train of short electron bunches each of charge q_b traverses a section of PETS l_s meters long, it builds up a voltage across the structure of peak value

$$U_f = \frac{\omega}{4}\left(\frac{R'}{Q}\right) l_s q_f \quad , \tag{3.1}$$

Where $\omega = 2pf$ is the excited mode frequency, R'/Q is the normalized longitudinal impedance per unit length (expressed in linac Ω/m) of the structure at frequency f, q_f is the total beam charge in one fill time T_f of the structure and l_s is the structure length. The fill time is simply the time it takes for the energy deposited by one bunch in the fundamental mode to travel through the structure: where β_g is the normalized group velocity.

$$T_f = \frac{l_s}{c}\frac{1}{\beta_g} \quad \text{where} \quad \beta_g = \frac{v_g}{c} \quad \text{is the normalized group velocity.}$$

In order for the mode excitation to be coherent and therefore constructive, the bunch spacing must be a multiple of the mode wavelength which is 10 mm and the mode phase velocity must be equal to the speed of the relativistic bunches. The bunch time separation T_b, however, must be much shorter than one fill time T_f, so that several bunches contribute to the build up of the voltage U_f. The rate of energy deposition by the beam or the RF power generated in the PETS is obtained by multiplying the voltage U_f by the average beam current in one filling time q_f/T_f:

$$P = \frac{\omega}{4}\left(\frac{R'}{Q}\right)\frac{{q_f}^2}{T_f} l_s F^2(\sigma) \quad . \tag{3.2}$$

The power form factor $F^2(\sigma)$ takes into account the finite length of the Gaussian bunches. For a train of bunches lasting much longer than the structure filling time, the peak power level in Eq. (3.2) stays constant provided that the charge per filling time remains constant. Expression (3.2) therefore gives the steady-state power level at the structure output when the internal wall losses are neglected.

3.5.2.3 The four-waveguide PETS

Structure parameters

Table 3.2 shows the main geometric and RF parameters of the transfer structure with a 26 mm beam chamber aperture which has been adopted as power extracting structure for the drive-beam decelerator [3.28].

Table 3.2: Parameters of the four-waveguide PETS

Beam chamber diameter	**26.00 mm**
Waveguide width	**8.60 mm**
Waveguide height	**4.00 mm**
Slit aperture	**7.00 mm**
Synch. mode frequency	**29.985 GHz**
Synch. mode b g	**0.441 c**
Synch. mode R ¢ /Q	**41.0 linac W /m**
Peak transverse wakefield	**0.22 V/pC/mm/m**
Transverse mode Q -value	**140**
Effective structure length	**0.80 m**
Nominal output power*	**530.4 MW**

PETS integrated longitudinal electric field uniformity

Because of the particular geometry of the PETS, the integrated decelerating field varies as a function of the angular and radial position within the beam chamber. In particular the integrated field increases as one moves towards the waveguides, while it decreases to zero towards the chamber walls. The non-uniform beam deceleration causes the particles to receive transverse kicks, which are functions of the particle position within the PETS chamber. The overall result found in tracking programs is that the drive beam would be unstable if no cure were found for the problem. One possible simple solution consists in rotating by 45 degrees every other PETS in the decelerating linac so that a particle off-centre at $\varphi = 0$ in a structure would be at $\varphi = 45$ degrees in the following one, thus averaging out the field non-uniformity. The useful effect of the alternate PETS rotation is somewhat reduced by the betatron motion of the particles in the drive linac lattice. Tracking programs have shown, however, that the overall result is beneficial to the transverse beam stability and worth the implementation effort [3.28].

3.6 Power transfer efficiency

One of the most important features in a high-energy linear collider is the power transfer efficiency. A list of efficiencies for different components of the design

considered is shown in Table 3.12, although it is too early to know the precise values for all of the subsystems. The target efficiencies are listed in the Table together with the more conservative values which have been assumed in the present report. Figure 3.8 shows the power flow of the whole CLIC complex, from the wall plug to the main beam.

This diagram does not take into account the power needed for the cooling of the beam dumps, of the accelerating structures, and of all the other components. Typically, direct cooling with water consumes about 3% of the dissipated power, while air-cooling is more expensive (about 40%). Assuming the use of water cooling whenever possible without additional costs, one obtains an additional wall-plug power of about 16 MW (280 MW water-cooled, i.e. 8.4 MW consumption, plus 20 MW air-cooled, corresponding to 8 MW consumption). The total installed cooling capacity (cooling towers) naturally does not need to be larger than the total wall-plug power, but depending on the specific mode of operation, the water flow may need to be shunted to particular loads or dumps. This requires a redundant plumbing, a cooling control, and an interlock system. Each installed load must be able to handle the maximum power possible at this location [3.30]. Another issue, which is not covered here, is the need for some operational overhead in the drive-beam accelerator. Additional klystrons could be needed for a fast substitution of failing tubes. If these klystrons feed structures permanently installed in the beam line, they should constantly provide power to compensate for the local beam loading. Depending on the expected failure rate and on the scenario chosen for the overhead, the additional power needed could be as high as 40 MW [3.30].

Table 3.3. Power efficiency % of the CLIC TBA multi TeV collider

Item		Assumed	Target
Modulator	η_M	90	92
Klystron	η_K	65	70
drive-beam acceleration*	$\eta_S \eta_A$	93	94
Decelerator	$\eta_{D,extr}$	82	85
Power extraction	η_{PETS}	95	97
Power transfer	η_{transf}	95	97
Wall plug to RF	$\eta_{plug/RF}$	40.3	48.4
RF to main beam	$\eta_{RF/main}$	24.4	24.4
Overall	η_{tot}	9.8	11.8

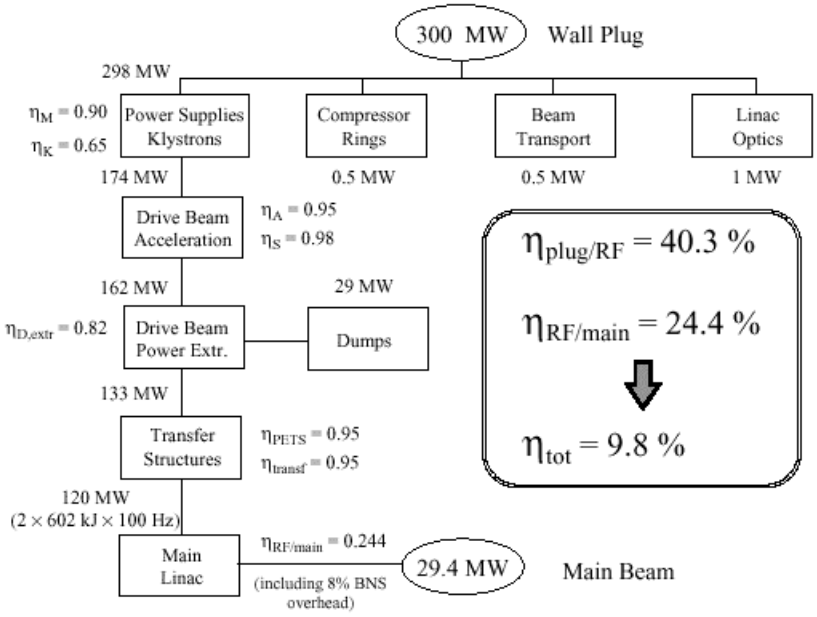

Figure 3.8. Power flow of the CLIC scheme

Reference:

Introduction (Section 3.1)

[3.1] A.M. Sessler, The FEL as a power source for a high gradient accelerating structure, AIP Conf. Proc. 91 (Ed. P.J. Channel), p. 154 (1982).

[3.2] H.H. Braun et al., The CLIC RF Power Source. A Novel Scheme of Two-Beam Acceleration for Electron–Positron Linear Colliders, CERN 99–06 (1999).

[3.3] R. Corsini and J.-P. Delahaye, The CLIC multidrive-beam scheme, CERN/PS 98–008 (LP) (1998) and CLIC Note 331 (1998).

Drive-beam injector (Section 3.2)

Overview of the system (Section 3.2.1)

[3.4] L. Rinolfi, O. Kester and R. Rao, Beam emittance measurements from CERN thermionic gun, Proc. 3rd Eur. Part. Accel. Conf. (EPAC92), Berlin, 1992, Eds. H. Henke, H. Homeyer and C. Petit-Jean-Genaz (Edition Frontières, Gif-sur-Yvette, 1992) and CERN/PS/92–12 (LP) (1992).

Beam dynamics simulations (Section 3.2.3)

[3.5] B. Mouton, The PARMELA program, Report LAL-SERA 93–455, Laboratoire de l'Accélérateur Linéaire, Orsay, France (1993).

Drive-beam accelerating linac (Section 3.3)

The accelerator beam dynamics (Section 3.3.1)

[3.6] K. Bane, M. Timm and T. Weiland, DESY-M-97-02 (1997).
[3.7] L. Thorndahl *in* H.H. Braun et al., The CLIC RF Power Source, CERN 99–06 (1999).
[3.8] D. Schulte, Stability of the CLIC drive-beam accelerator, Proc. 19th Int. Lin. Accel. Conf. (LINAC'98), Chicago, 1998 and CERN-PS-98–042-LP (1998).
[3.9] D. Schulte, The Drive-Beam Accelerator of CLIC, Proc. of VIIIth Int. Workshop on Linear Colliders (LC99), Frascati, 1999, Eds. J.-P. Delahaye, G. Guignard, K. Hübner et al., URL:
http://wwwsis.lnf.infn.it/talkshow/
lc99/Schulte2b/talk.pdf

Description of the accelerator cavities (Section 3.3.2)

[3.10] M. Luong, private communication.
[3.11] R.H. Siemann, Linear colliders: the last ten years and the next ten years, SLAC-PUB-6417 (1994).
[3.12] L. Thorndahl, private communication.

Drive-beam power systems (Section 3.3.3)

[3.13] A. Beunas, Thomson Tubes Electroniques, Paris, private communication.
[3.14] P.D. Pearce et al., A klystron-modulator RF power system for the CLIC drive-beam accelerators, 24th International Power Modulator Symposium, Norfolk, Virginia, June 2000.

Frequency multiplication and pulse compression (Section 3.4)

Design of the delay line and combiner rings (Section 3.4.1)

[3.15] J.B. Murphy, S. Krinsky and R.L. Gluckstern, *Longitudinal wakefield for an electron moving on a circular orbit*, Part. Accel. **57** (1997) 9.
[3.16] L. Thorndahl, private communication.
[3.17] G. Guignard and E.T. D'Amico, A new family of isochronous arcs, CERN/SL 95–24 (AP) and CLIC Note 280 (1995).
[3.18] R.C. York and D.R. Douglas, Optics of the CEBAF CW superconducting accelerator, Proc. 12th Particle Accelerator Conference, Washington, DC, 1987 (IEEE, New York, 1987).
[3.19] Ph. Bernard, H. Lengeler and V. Vaghin, New Disk-Loaded Waveguides for the CERN RF Separator, CERN 70–26 (1970).

Transfer lines, compressors, path-length chicanes and loops (Section 3.4.2)

[3.20] E.T. D'Amico and G. Guignard, Tunable achromats and CLIC applications, Proc. EPAC2000, Vienna, June 2000.

Drive-beam decelerator (Section 3.5)

Lattice and beam stability (Section 3.5.1)

[3.21] A. Riche, Maximum energy transfer efficiency in CLIC drive beam and proposal for a method of focusing, CLIC Note 266 (1994)
[3.22] A. Riche and D. Schulte, The drive-beam decelerator of CLIC, Proc. 19th Int. Lin. Accel. Conf. (LINAC98), Chicago, 1998 and CERN-PS 98–043-LP (1998).
[3.23] A. Riche, To be published.
[3.24] D. Schulte, PLACET: a program to simulate drive beams, Proc. EPAC2000, Vienna, June 2000.
[3.25] A. Millich, A. Riche and D. Schulte, Beam stability in the CLIC drive-beam decelerator using structures of high-order symmetry, Proc. Part. Accel. Conf. (PAC99), New York, 1999, Eds. A. Luccio and W. MacKay (IEEE Computer Soc. Press, Piscataway, N. J., 1999) and CERN-PS 99–028-LP (1999).

The Power Extraction and Transfer Structure (Section 3.5.2)

[3.26] W. Schnell, The study of a CERN linear collider, CLIC, Linear Accelerator Conference, Williamsburg, 1988.
[3.27] G. Carron and L. Thorndahl, Impedance and loss factor measurements on a CLIC Transfer Structure (CTS), Proc. 3rd Eur. Part. Accel. Conf. (EPAC92), Berlin, 1992, Eds. H. Henke, H. Homeyer and C. Petit-Jean-Genaz (Edition Frontières, Gif-sur-Yvette, 1992).

[3.28] G. Carron, A. Millich and L. Thorndahl, The 30 GHz transfer structure for the CLIC study, International Computational Accelerator Physics Conference (ICAP 98), Monterey, 1998.
[3.29] M. Luong and I. Syratchev, Simulations of the damping of the power extraction and transfer structure, Proc. EPAC2000, Vienna, June 2000.

Power transfer efficiency (Section 3.6)

[3.30] R. Pitthan, private communication.

4 CLIC Test Facilities and the Route to CLIC

4.1 The various stages and a possible schedule

The basic principles of the two-beam acceleration technique have been established in the first two CLIC test facilities, i.e. CTF1 [4.1], which is now out of operation, and CTF2 [4.2], which is still running. It is now proposed to demonstrate the overall feasibility of the many key issues, which are specific to the CLIC scheme in two distinct successive stages. The first stage, which would take five years, would be to build and exploit a new test facility (CTF3) which would demonstrate the feasibility, and test all the critical components of the RF power generation scheme albeit on a much smaller scale and with the drive linac at a different (higher) frequency. This facility would be housed in the

present LPI (LIL+EPA) buildings. The second stage, which would come immediately after CTF3 and which would take about five years, would be to build a limited, first-phase version (CLIC1) of the real CLIC power source to produce just one single-drive-beam unit rather than the multiple drive-beams it would ultimately be required to produce. This drive-beam would have the nominal CLIC energy and current, and would provide enough power in a ~ 624 m long section of the CLIC linac to accelerate a multibunch beam to 68 GeV. Since this is a final test of the CLIC scheme, all components will be definitive ones and, given a positive outcome of the test, would be used for the final construction.

4.2 CLIC Test Facilities

4.2.1 CTF1 overview and results

The technical feasibility of two-beam acceleration was first demonstrated in the CLIC Test Facility CTF1 [4.1] which was built to (i) study the production of short, high-charge electron bunches from laser-illuminated photocathodes in RF guns, (ii) generate high-power 30 GHz RF pulses by passing bunch trains through energy extraction cavities for testing CLIC prototype components, (iii) test beam-position monitors. A layout of CTF1 is shown in Fig. 5.1. A 3 GHz 1.5-cell RF gun equipped with a laser-driven photocathode and operating at 100 MV/m produced a bunched beam with a momentum of 4.5 MeV/c. A solenoid at the outlet of the gun provided some focusing of the beam before it was

accelerated to 12 MeV/*c* in a four-cell standing wave gun-booster cavity. Final acceleration to 65 MeV/*c* was obtained using a 1 m long travelling-wave section — provided by LAL. Energy was extracted from the beam by a 30 cm long travelling-wave section (CAS1) to provide short high-power 30 GHz RF pulses. This power was in turn fed to a second identical CLIC structure (CAS2) to produce high accelerating gradients. The decelerated beam then either went to a dump, or was turned through 180° by bending magnets at the end of the line and re-accelerated by the second high-gradient CLIC section. The facility was operated in either single-bunch or multi-bunch mode at a repetition rate of 10 Hz. Multiple bunches were made by splitting the laser pulse into a train of pulses each spaced by one 3 GHz wavelength. The synchronized laser system had been optimized at the fourth harmonic (262 nm) providing a maximum energy of 0.5 mJ per pulse (before splitting) and a pulse length of 8 ps FWHH. After an initial period of operation with CsI photocathodes, Cs_2Te photocathodes were later used. These photocathodes were prepared in the laboratory and transported under vacuum and installed in the gun using a specially designed transfer system. The RF gun produced 35 nC in a single bunch and 450 nC in a train of 48 bunches. Only a small fraction of this charge, however, could be transported to the dump. The maximum 30 GHz RF power produced was 76 MW for 3 ns. The highest average accelerating field in the second CLIC accelerating structure was 94 MV/m.

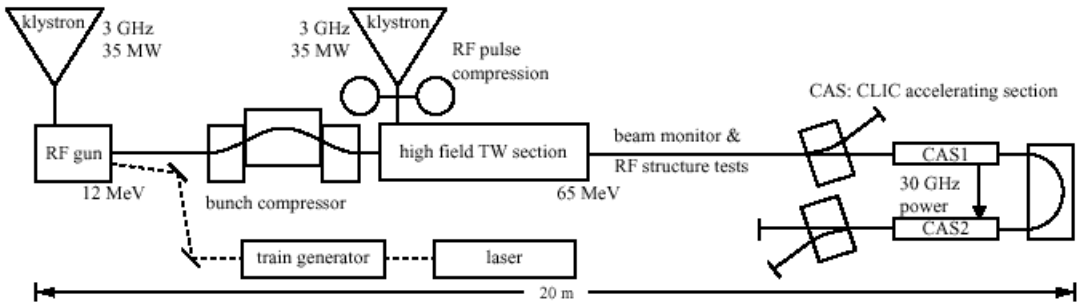

Fig. 4.1 : Layout of the facility CTF1, which is now out of operation.

4.2.3 CTF3 description

Since CLIC1 is a very large and expensive installation, a much smaller facility (CTF3) [4.3] is proposed as a first intermediate step to demonstrate the technical

feasibility of the key concepts of this new RF power source, e.g., generation of interleaved bunch trains, operation with a fully-loaded drive-beam accelerator, and generation of accelerating gradients of 150 MV/m. The new CLIC Test Facility (CTF3) is shown in Fig. 4.2. To reduce costs, CTF3 differs from the RF power source proposed for CLIC in the following ways (Table 4.1). The frequency of the drive-beam accelerator is chosen to be 3 GHz instead of 937 MHz. This enables the 3 GHz klystrons, modulators, RF power compression units, and waveguides from the LEP Injector Linac (LIL) Complex to be used for power production which is always very costly. With 10 of these modulator/klystron units the drive-beam energy for a current of 3.5 A (~ half the nominal CLIC current) is 184 MeV — this is very low compared to the 1.18 GeV for CLIC and obviously makes operation more difficult, but simulations indicate that it works. CTF3 only has the first two stages of the beam combination scheme, namely the times-2 Delay Line Combiner and the first Combiner Ring. The second (´4) large circumference Combiner Ring is very expensive and since it has the same scheme of combination it is not considered to be essential for this first demonstration test facility. The compression factor for the first Combiner Ring has, however, been increased from 4 for CLIC, to 5 for CTF3, to obtain an overall compression of 10. This gives a final bunch spacing of 2 cm (the same as in CLIC) for production of power at 30 GHz. Because of space limitations, it is unlikely that the circumference of the Combiner Ring can be made smaller than 84 m. This results in a final pulse length of 140 ns rather than the nominal CLIC value of 130 ns. The modulators produce a maximum RF pulse of 6.7 μs which after power compression with LIPS (´2.3) becomes ~1.6 μs. This beam pulse is long enough after a (´10) frequency multiplication to produce the required final 140 ns pulse. The drive-beam decelerator is limited to a total length of about 10 m (four transfer structures) compared to 624 m for CLIC. To limit the radiation produced by CTF3 it is proposed to run at 5 Hz instead of 75 Hz. The new facility will be housed in the existing LIL and EPA buildings and use will be made of many of the LIL and EPA components. As mentioned above, an 84 m circumference ring appears just to fit in the EPA.

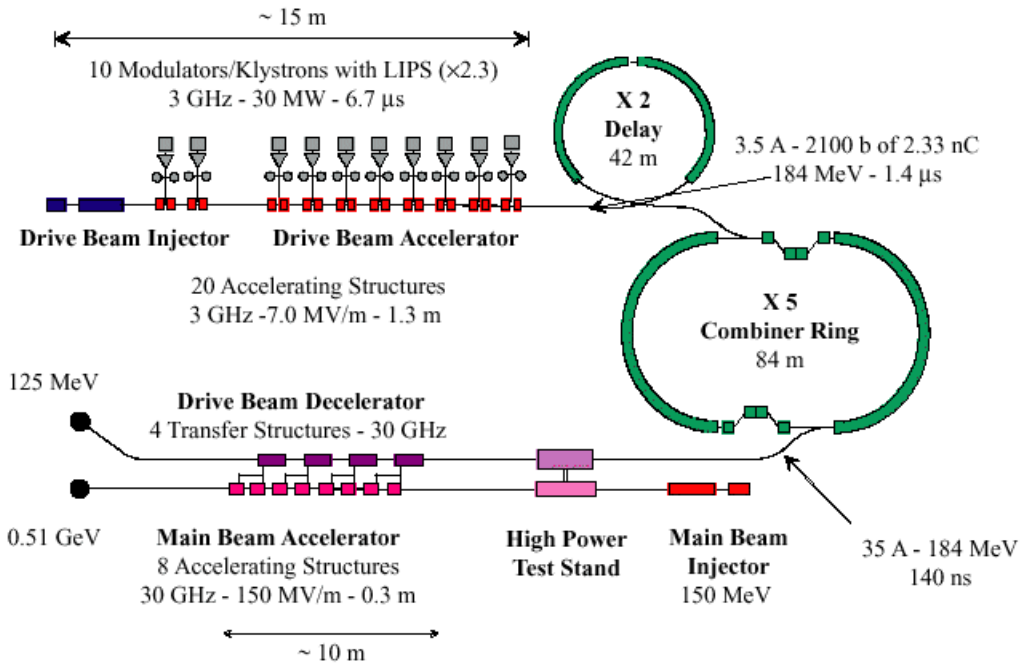

Fig. 4.2: *Schematic layout of nominal phase of CTF3.*

Table 4.1 : Comparison of CTF3, CLIC1 and CLIC (3 TeV) parameters

		CTF3	CLIC1	CLIC
Accelerating frequency	(GHz)	30	30	30
Main linac accelerating gradient	(MV/m)	150	150	150
Number of accelerating structures per linac		8	976	22×976
RF pulse length	(ns)	140	130	130
Main beam acceleration per drive beam	(GeV)	0.36	68	68
Number of transfer structures per linac		4	488	22×500
Number of drive beams per linac		1	1	22
Frequency of drive-beam accelerator	(MHz)	3000	937	937
Drive-beam energy	(MeV)	184	1180	1180
Average drive-beam current before compression	(A)	3.5	7.5	7.5
Number of klystrons		10	46	182
Number of RF power compressors		10	46	0
Drive-beam pulse length before compression	(µs)	1.40	4.16	92
Interval between bunches before compression	(cm)	20	64	64
Delay line combiner		42 m (×2)	39 m (×2)	39 m (×2)
First combiner ring		84 m (×5)	78 m (×4)	78m (×4)
Second combiner ring		NO	312 m (×4)	312 m (×4)
Overall frequency multiplication		10	32	32
Final average drive-beam current after compression	(A)	35	240	240
Interval between bunches	(cm)	2	2	2
Drive-beam energy per pulse	(kJ)	0.8	37	814
Repetition frequency	(Hz)	5	100	100
Average beam power	(kW)	4.1	3690	81×10^3
Drive-beam energy on beam dump	(MeV)	125	118	118

References

[4.1] K. Aulenbacher et al., Results from the CLIC Test Facility (CTF1), CERN/PS/96-28 (LP) and CLIC Note 310 (1996).
[4.2] H.H. Braun for the CTF Team, Experimental results and technical research and development at CTF2, Proc. 7th Eur. Part. Accel. Conf. (EPAC2000), Vienna, 2000.
[4.3] CLIC Study Team, Proposals for future CLIC studies and a new CLIC Test Facility (CTF3), CLIC Note 402 (July 1999).